Computational and experimental evidence that auxin accumulation in nodule and lateral root primordia occurs by different mechanisms*

Eva E. Deinum[†‡] René Geurts[‡] Marijke Hartog[‡]
Ton Bisseling[‡] Bela M. Mulder[†§]

Abstract

The formation of root lateral organ formation typically requires the *de novo* generation of a primordium, initiated at the site of local auxin accumulation. Legume roots are a particular interesting example in this respect, as they can give rise to both lateral roots and root nodules. The initiation of the latter primordium is much less understood. Using computer simulations we start with an unbiased comparison of different mechanisms that a priori seemed capable of producing local auxin accumulation. These mechanisms all produce different characteristic signatures, of which a reduction of auxin efflux best matched the morphology of nodule primordia. This lead to the prediction that root nodule positions would not be affected by root curvature – contrary to lateral root primordia, that are initiated by increased influx – which we experimentally confirmed. We further investigate how changes in the *in silico* root segment affect the induction and shape of local auxin maxima and discuss the functional implications of these findings with respect to nodule type and bounding the developmental zone where nodulation takes place.

1 Introduction

The plant body plan is highly adaptive: new organs are created according to need. Legume roots form a particular interesting example with respect to lateral organ initiation: they can form different types of organs, lateral roots

*Chapter 66 of *Biological Nitrogen Fixation, Volume 2*, First Edition. Edited by Frans J. de Bruijn. Publisher: John Wiley & Sons, 2015

[†]FOM Institute AMOLF, Amsterdam, The Netherlands

[‡]Laboratory for Molecular Biology, Department of Plant Sciences, Wageningen University, Wageningen, The Netherlands

[§]Laboratory for Cell Biology, Department of Plant Sciences, Wageningen University, Wageningen, The Netherlands

and root nodules. Although the latter are initiated in response to rhizobium-secreted signaling molecules, Nod factors, and the primordia of the two types originate in different cell layers, accumulation of the plant hormone auxin at the site of primodium initiation occurs in both [Rolfe et al. 1997, Larkin et al. 1996, Mathesius et al. 1998, Pacios-Bras et al. 2003, Takanashi et al. 2011]. Given the importance of this hormone in the process, it is not surprising that the number of lateral roots can be increased by exogenous auxin application [Blakely and Evans 1979, Woodward and Bartel 2005]. This is, however, not reported for root nodules. Auxin's textbook antagonist, cytokinin, on the other hand, can be used to induce nodule like structures [Cooper and Long 1994], as can auxin transport blockers [Hirsch et al. 1989]. A cytokinin receptor is essential for nodulation [Gonzalez-Rizzo et al. 2006, Tirichine et al. 2007, Murray et al. 2007, Plet et al. 2011] and cytokinin response regulators are activated early in the process [den Camp et al. 2011]. This further demonstrates the importance of this hormone in nodulation. On lateral roots, however, it has an inhibiting effect [Laplaze et al. 2007]. Auxin efflux carrier PIN1, which is upregulated in lateral root formation, is readily removed from the plasma membrane of primordium cells upon cytokinin addition [Marhavy et al. 2011].

This paradox suggests that the mechanisms underlying auxin accumulation in lateral root and root nodule primordia differ, for which we offer additional experimental evidence. We hypothesize that the Nod factor activated cytokinin signaling causes local auxin accumulation in the cortical layers that form the nodule primordium. We start with an unbiased analysis of three conceptually different mechanisms for local auxin accumulation. From this we continue with the best candidate and discuss the likelihood that cytokinin can trigger the proposed mechanism.

To date, the formation of **lateral roots** has been studied most extensively in the model organism *Arabidopsis thaliana*. The lateral roots of these plants originate exclusively from a few pericycle cells, the "founder cells" [Malamy and Benfey 1997, Casimiro et al. 2003]. These cells are the site of the first auxin accumulation [Hirota et al. 2007]. In model legumes, which, contrary to *Arabidopsis*, all have a multi-layered cortex, the lateral root primordia are also predominantly of pericycle origin [Mallory et al. 1970] and the first auxin accumulation is observed in the pericycle [Rolfe et al. 1997, Larkin et al. 1996].

The formation of **root nodules** starts with an encounter of a compatible Rhizobium bacterium, which is recognized by the plant host through the species specific Nod factors it produces [Jones et al. 2007]. Two major types of legume nodules are found on the model species: determinate and indeterminate, named after the persistence of a meristem only in the latter [Hirsch 1992]. One model legume, *Lotus japonicus*, forms determinate and the other, *Medicago truncatula*, forms indeterminate nodules. Interestingly,

the primordia of determinate nodules originate in the outer to middle cortical layers, whereas the indeterminate primordia originate from the inner cortical layers [Hirsch 1992]. Correspondingly, local auxin accumulation has been found at the sites of the first cortical cell divisions in lotus [Pacios-Bras et al. 2003, Takanashi et al. 2011] and white clover (indeterminate) [Mathesius et al. 1998].

Lateral roots and root nodules originate in approximately the same zone of the legume root. For nodules this is called the susceptible zone [Bhuvaneswari et al. 1981]. In the youngest part of this zone the epidermal cells start developing root hairs. Cortical cells in the zone have fully differentiated and in the process of nodule formation they will de- and redifferentiate. Throughout this text we sometimes refer to the legume susceptible zone using "DZ" (standing for 'differentiation zone"), thereby stressing the origin of the parameters we use (see methods).

Auxin is active in minute concentrations [Ljung et al. 2001, Marchant et al. 2002, Petersson et al. 2009]. The most abundant natural auxin, Indol-3-acetic acid (IAA) is a weak acid with $pK_a \approx 4.8$. Its protonated form, IAAH, can passively cross the cell membrane, which is, however, practically impermeable to the deprotonated form, IAA^-. Because the apoplastic is slightly acidic and the cytoplasm neutral, this difference can result in an influx of auxin against the total auxin concentration [Mitchison 1980, Steinacher et al. 2012]. This influx can be enhanced by more than an order of magnitude by auxin influx cariers such as the AUX1/LAX family [Swarup et al. 2005]. These are typically located homogeneously over the cell membrane, or at increased levels at the apical and basal sides of the cell [Swarup et al. 2001; 2004, Kleine-Vehn et al. 2006]. Efflux occurs predominantly by efflux carriers such as the PIN proteins [Galweiler et al. 1998, Paponov et al. 2005], often concentrated on specific sides of the cells. This gives rise to directional auxin transport [Benkova et al. 2003, Blilou et al. 2005]. For an excellent review on auxin biosynthesis we refer to [Mano and Nemoto 2012]. Because no tools exist yet for live monitoring the auxin concentration in living plants, computer models have become an indispensable tool in studying the many roles of this plant hormone in plant development – see [Kramer 2008, Grieneisen and Scheres 2009, Garnett et al. 2010, Jonsson and Krupinski 2010] for some reviews.

From this overview of auxin transport and metabolism we arrive at three major scenarios for increasing the auxin concentration in a cell: increasing the amount of influx carriers, decreasing the amount of efflux carriers and local auxin production [Deinum et al. 2012]. We use a computational model of a generalized legume root segment to investigate the possibilities of inducing local auxin accumulation through these mechanisms and their distinguishing properties. For this we apply these scenarios to a designated part, the "**controlled area**" of an *in silico* root segment. We find that the three scenarios all yield different spatial and spatio-temporal signatures. Of these,

the signature generated by a reduction of the efflux was most compatible with the observed patterns of auxin accumulation and the morphology of the nodule primordium. Because this differs from the mechanism of lateral root primordium initiation, we expect root nodule positioning lacks the sensitivity to root curvature found in lateral roots, which we experimentally verify. The lateral position of the cortical auxin maximum can be shifted by small changes in the distribution of cortical PIN proteins. Based on this observation we discuss the possibility that cortical PINs determine the lateral position of the first cell divisions in nodulation, which in turn is correlated with the type of nodules produced.

2 Methods

2.1 Simulations of auxin transport and metabolism in root segments

Auxin transport and metabolism are modelled with subcellular precision. Within a cell and inside the apoplast, auxin moves by diffusion with diffusion constants D_C and D_W, respectively. Transport over the cell membrane is modelled using directional effective permeabilities P_{in} and P_{out} for influx and efflux. This implicitly assumes non-saturating processes or carriers operating far from saturation. This results in flux over the membrane (positive means outward flux): $J_{mem} = P_{out}C_c - P_{in}C_w$. In our simulations, efflux parameter P_{out} can be set for each cell face independently, whereas influx parameter P_{in} is always the same for all four faces of the cell. Parameters and default values are summarized in **table 1**. Further details of the simulations in [Deinum et al. 2012].

Lacking data on PIN positioning in the relevant root of a real model legume, the PIN layout was based on an experimentally founded model developed for *Arabidopsis* [Laskowski et al. 2008], geometrically adopted to resemble model legumes *Medicago* and *Lotus* [Deinum et al. 2012].

The simulation root segments we used are much longer than the region of interest, as to minimize effects from the boundaries. Boundary conditions and motivation are further described in [Deinum et al. 2012].

2.2 Changes applied in the "Controlled Area"

A designated part of the root segment (**fig. 1AB**), a 0.5 mm block comprising epidermis and cortex on one side of the root, is designated "**Controlled Area**". All scenarios are implemented as a change applied to these cells: (n-fold) increase of the effective influx permeability, (n-fold) Infl↓, (n-fold) decrease of the effective efflux permeability, (n-fold) Effl↓, and local auxin production with a given rate, Prod↑.

2.3 Concentrations are normalized with respect to the vascular tissue

For easier interpretation of the results we have normalized the concentration in the root segments with the average vascular concentration in a segment without any change in the controlled area. This level we call C_v. Thus, a concentration of $2C_v$ means twice as much auxin than the average for the vascular tissue. Where applicable, auxin production occurs with rate p in normalized concentration units per second per unit of volume.

2.4 Plant growth and gravitational stimulation

7-8 *Medicago truncatula A17* seedlings were grown on each 24x24 cm plate with Buffered Nod medium containing AVG. The plants' gravitational field was changed by 90 degree turning of the plates at irregular 1-3 day intervals. Upon transfer to the plates they were inoculated with rhizobium strain *Sinorhizobium meliloti 2011* and covered by transparent sheets to ensure continued contact with the medium. Medium, seed treatment and germination according to standard protocols `www.noble.org/medicagohandbook`.

2.5 Statistical methods

All statistical calculations were made using self-written scripts. For comparison of fractions of lateral organs on curved vs. straight parts we calculated $p = \int_{q=0}^{1} P(f_L \leq q \wedge f_N = q)\mathrm{d}q$, with f_L and f_N the "true" fraction of lateral roots or nodules, respectively, on curved regions of the roots on a particular plate. Probability density functions for f_L and f_N were calculated based on binomial distributions: $P(f_L \leq q) = \frac{1}{I_0} \int_{r=0}^{q} \binom{n}{c} r^c (1-r)^{n-c} \mathrm{d}r$, with c the number of lateral roots on curved parts of the root out of a total of n observations and I_0 the total mass of the integral. With this statistic, $p = 0.5$ means that nodules and lateral roots are equally likely to appear in curved regions. As the fraction of root length that qualifies as curved differs among plates, all comparisons were made within plates only.

3 Results and Discussion

3.1 Different mechanisms for local auxin accumulation leave different signatures

From the available knowledge on auxin transport and metabolism we have selected three conceptually different mechanisms that could in theory lead to local auxin accumulation: Infl↓, Effl↓ and Prod↑ [Deinum et al. 2012]. We investigated the behaviour of these mechanisms in an *in silico* root segment representative of the susceptible zone of a model legume (**fig. 1AB**). The

PIN layout of this root segment results in a rootward auxin flux in the stele and a shootward flux in the cortex.

Figure 1: Different mechanisms for local auxin accumulation leave different signatures.

An increase of the effective influx permeability, Infl↓, resulted in an increase of the auxin concentration in the controlled area (**fig. 1C**). This increase, however, was strongest on the left side of the controlled area, which is its downstream side with respect to the cortical auxin flux. This strong focus on the downstream side occurred independent of the length of the controlled area (data not shown).

With a decrease of the effective influx permeability, Effl↓, on the other hand, we observed a broad auxin accumulation pattern (**fig. 1D**). Although the concentration on the shootward side of the controlled area was slightly higher than on the rootward side, this bias was much weaker than with Infl↓.

With both Infl↓ and Effl↓, the minimal change for an increase of the maximum cortical concentration above the vascular level C_v was between 4-fold and 10-fold. Such levels were not reached with the local production scenario Prod↑ (**fig. 1E**). Regardless of the production rate the concentration in the controlled area remained far below $1C_v$. This could not be attributed to a too low production rate, as the highest rate we used should be considered high based on gas chromatography and mass spectroscopy measurements by Ljung et al. [2001] and Marchant et al. [2002]. Moreover, the absolute increase in the vascular tissue rootward, i.e. downstream, of the production site was higher than in the controlled area itself, demonstrating that the auxin was mostly transported away. This is in line with a proof-of-principle simulation (of the *Arabidopisis* root) by Grieneisen *et al.* in which the whole auxin maximum around the quiescent centre (QC) of the root tip could be filled by a single auxin producing cell, a distant cortical cell, that soon contained less auxin than cells near the QC and eventually contained almost the same concentration as the cortical cells surrounding it [Grieneisen et al. 2007].

These signatures did not rely on the regular alignment of the cell files and were robust against variations in cell length (**fig. 1F-H**).

From the different signatures we can conclude that the accumulation mechanism affects the dimensions of the resulting primordium. The DR5 data of auxin accumulation in lateral root primordia by Hirota et al. [2007] actually show an auxin maximum that is more focussed than the region where influx carrier AUX1 is upregulated.

The broad accumulation pattern found with the Effl↓ scenario seems most compatible with the experimental observation that nodule primordia are typically broader than lateral root primordia.

3.2 Lateral roots and nodules respond differently to gravitropically induced curvature

On curved roots, lateral roots typically emerge on the convex side ("outside") of the curved part [Fortin et al. 1989]. Moreover, lateral roots can be promoted by mechanical or gravitropical root bending [Fortin et al. 1989, Laskowski et al. 2008], the first induction method also demonstrated in *Medicago truncatula* [Lillo 2012]. Computer simulations by Laskowski *et al.* show that the geometrical effect of the bending results in a slight increase of the local auxin accumulation, particularly in the pericycle. This can be enhanced by auxin induced AUX1 expression, through a positive feedback between increased auxin accumulation and increased influx [Laskowski et al. 2008]. If the initial auxin accumulation in root nodule primordia is indeed caused by a reduction of the efflux, we expect that they do not show the typical distribution with respect to root curvature as seen in lateral roots.

To investigate this, we subjected *Medicago truncatula* plants to irregular gravitropic stimuli to induce highly curved roots. Nodule and lateral root positions were scored in three categories with respect to curvature: convex, concave and straight/unclear (**fig. 2**). In line with observations from other species, and mechanical root bending experiments in *Medicago*, lateral roots showed a very strong preference for the convex sides of roots (p=2.84e-10, p=1.42e-14, 2-tailed binomial test). Root nodules on the other hand showed no significant bias for either convex or concave side of the curved parts of the root (p=1, p=0.699, 2-tailed binomial test). Moreover, in both experiments, the percentage of lateral roots occurring in curved regions was larger than for root nodules on the same plants (42% vs. 26%, p=0.014 and 59% vs. 43%, p=0.011). This suggests that lateral roots are positively induced by root curvature, whereas nodules are not, or to much lesser extent. Not only is this entirely in line with our expectation based on the different mechanisms, it is also functionally relevant. Whereas the average result of lateral root formation on the convex side of root curves rather than the concave side is a larger occupied soil volume, the main functional requirement for nodule primordia is that they originate close to the initial infection site and not on the other side of the vascular bundle if the root happens to be curved.

Based on our results so far we continued our investigation with a strong focus on the Efflux scenario.

Figure 2: Root nodule position is insensitive to root curvature.

3.3 Auxin accumulation following efflux reduction starts closest to auxin sources

In **fig. 1** we investigated steady state patterns of auxin accumulation. A very relevant question is, therefore, whether the auxin accumulation occurs fast enough to be compatible with the know timing of nodulation events.

In other words, a sufficient increase in auxin concentration is needed at least several hours prior to the first cortical cell divisions. This boils down to a time window of at most 20 hours: at 18-24 hours after inoculation, the cortical cells show cytoskeletal signs of activation for division [Timmers et al. 1999] and no cortical cell divisions are observed within 20 hours after inoculation [Yang et al. 1994]. As our approach involves an instantaneous change in the transport parameters and no transcription or translation of regulatory genes, the actual maximum time window is probably a several hours shorter.

To check for compatibility, we followed the dynamics of auxin accumulation in the controlled area (**fig. 3**). With our default parameters, the steady state was reached much faster than necessary (**fig. 3AC**). Auxin accumulation was also fast enough when we slowed down all dynamics by reducing all effective influx and efflux permeabilities by a factor 10 (**fig. 3BD**). Also in the latter case enough time is left for processes we did not explicitly consider, such as the induction of the reduction of the efflux permeability and transcription of early nodulin genes. Such processes can happen fast, as most PIN1 disappears from the cell membrane in *Arabidopsis* lateral root primordia within one hour upon cytokinin treatment [Marhavy et al. 2011] and early nodulin gene ENOD40 is upregulated within 3 hours after spot inoculation in alfalfa [Compaan et al. 2001].

Figure 3: Auxin accumulation following an efflux reduction starts from the inner cortex, closest to the main auxin source.

By studying the time scales of auxin accumulation under Efflˇ in different modified roots and different factors of efflux reduction, Deinum *et al.* found that the time scales of auxin accumulation are determined by the time scales of redistributing auxin over the whole controlled area. This, in turn, is largely set by the remaining effective efflux permeability at the shootward side of the cortical cells, i.e., the side with most PINs, inside the controlled area [Deinum et al. 2012] (specially fig. 3).

Interestingly, the auxin accumulation after efflux reduction did not occur homogeneously throughout the controlled area. The first accumulation seen in the innermost cortical layer and also on the rootward (right) side of the controlled area (**fig. 3**). These two locations correspond to the vicinity of auxin sources: the vascular tissue with its high auxin concentration and from the shootward flux in the cortex, respectively. The temporal difference was most pronounced with the reduced parameters (**fig. 3BD**). See also [Deinum et al. 2012], fig. S2. As the auxin accumulation progressed, the transverse cortical concentration profile became flat again, just as in the root prior to induction.

3.4 Can cortical PINs make the difference between "indeterminate" (inner cortex) and "determinate" (middle-outer cortex) auxin accumulation?

A key difference between determinate and indeterminate is the radial position of the cortical cell divisions that form their primordia, and (most likely) the position of correlated auxin maximum. Determinate nodules originate from the middle to outer cortex, indeterminate nodules from the inner cortex [Pacios-Bras et al. 2003, Takanashi et al. 2011, Mathesius et al. 1998, Libbenga and Harkes 1973, Timmers et al. 1999]. In our simulations so far, we assumed an equal amount of PIN proteins in the central and peripheral lateral membranes of the cortical cells. This resulted in an auxin maximum that was homogeneous in the radial direction (* in **fig. 4**). We then investigated whether a central-peripheral bias in the effective efflux permeabilities could shift radial position of the Efflˇ auxin maximum and how strong such a bias would have to be.

For this we designed new reference segments with different inward and outward effective efflux permeabilities of the lateral cell membranes of all cortical cells and applied Efflˇ to all of those (**fig. 4**). Already the smallest biases we tried, amounting to 20% more or 20% less outward than inward efflux, produced a marked radial shift of the auxin maximum in the controlled area and even with the strongest inward bias the maximum concentration in the controlled area was well above the vascular concentration C_v.

Figure 4: Changes in cortical PINs can shift the lateral location of the induced cortical auxin maximum.

Neither the formation of determinate, nor the formation of indeterminate nodules defines a monophyletic group within the legumes [Doyle 1994, Mergaert et al. 2003]. This suggests that the transition between different nodules is relatively easy on evolutionary time scales. Moreover, grafting experiments show that the distinguishing feature must be root autonomous [Lohar and VandenBosch 2005]. Based on our results and the strict assumption that maximum auxin accumulation predicts the cell division site and through that nodule type, we tentatively hypothesize that slight changes in the lateral bias of PIN positioning could be such an "easy" change at the root of nodule type differentiation. A candidate system that could foster such changes would be the differential regulation of PINOID and/or PP2A activity, which play an important role in the polar positioning of PIN proteins through their phosphorylation and dephosphorylation, respectively [Friml et al. 2004, Michniewicz et al. 2007]. In a different context, changes in PINOID activity affected the central-peripheral PIN distribution [Ding et al. 2011].

3.5 PIN layout: co-determinant of the susceptible zone through controlling cortical auxin availability?

As the root develops, cells elongate and differentiate [Dello Ioio et al. 2008, Dolan et al. 1993] and also the distribution of PIN proteins over the different cell faces changes [Laskowski et al. 2008]. In the original *Arabidopsis* model the root is divided into three major zones. Starting from the root tip, these are: MZ ("meristematic zone"), EZ ("elongation zone") and DZ ("differentiation zone") [Laskowski et al. 2008]. The susceptible zone for nodulation is most similar to the DZ with respect to geometry and developmental stage, as root hairs, the canonical rhizobial entry point, arise in the DZ. This made the DZ a very natural starting point of our simulation study. We wondered, however, whether other factors could also affect if and how easily lateral organs could be induced in particular root zones. We, therefore, investigated the effects of Infl↓ and Effl↓ using the EZ PIN layout (**fig. 5I**).

Interestingly, the same changes that produced large auxin accumulation in the default (DZ) segment (**fig. 5CD**), had apparently little effect in the EZ segment (**fig. 5KL**). Upon closer inspection, the radial concentration profiles in the controlled area were similar to those without any change (**fig. 5E-H**). This shows that the propensity for auxin accumulation in the controlled area strongly depends on the cortical auxin availability, which is much larger in the DZ (**fig. 5B**) than the EZ (**fig. 5J**) segment.

Figure 5: Local auxin accumulation in different zones of the root

In the radial direction, the only difference between the EZ PIN layout – which shows markedly little auxin accumulation – and the rightmost segment of **fig. 4** – which showed a strong auxin accumulation in the inner cortex – is in the endodermis. This suggests that a strong inward (or "L-shaped") PIN distribution in the endodermis could reinforce the distal boundary of the susceptible zone through a strong reduction of the amount of auxin available in the cortex. We like to add that also the appearance and elongation of root hairs are stimulated by auxin [Masucci and Schiefelbein 1994, Pitts et al. 1998], so the same change of endodermal PIN positioning most likely has a double and congruent effect on specifying the susceptible zone in many legumes.

4 Conclusion and Outlook

To shed light on the earliest stages of root nodule formation and the role of auxin therein, we have investigated conceptually different mechanisms for local auxin accumulation in roots. These mechanisms all show their own characteristic signatures. Of the mechanisms investigated, a reduction of efflux was most compatible with diverse experimental observations. This is a different mechanism from the increased influx that is key to lateral root formation, predicting a different sensitivity of lateral root and root nod-

ule formation to root curvature, which we subsequently observed *Medicago* plants upon gravitropic stimulation. The simple approach taken here, of course, has its limitations, which marks the mechanism of their induction as an important topic for follow-up investigations. Further computational studies could also help identify downstream consequences of our tentative hypothesis on different PIN distributions in relation to nodule type that are easier to address experimentally.

5 Acknowledgements

The work of EED is funded within the research program of the Netherlands Consortium for Systems Biology (NCSB), which is part of the Netherlands Genomics Initiative (NGI)/NWO, RG is funded by NWO VIDI grant 864.06.007 and the work of BMM is part of the research program of the "Stichting voor Fundamenteel Onderzoek der Materie (FOM)," which is financially supported by the "Nederlandse Organisatie voor Wetenschappelijk Onderzoek (NWO)."

References

Benkova E, Michniewicz M, Sauer M, Teichmann T, Seifertova D, *et al.* 2003. Local, efflux-dependent auxin gradients as a common module for plant organ formation. *Cell* **115**, 591–602.

Bhuvaneswari TV, Bhagwat AA, Bauer WD 1981. Transient susceptibility of root cells in four common legumes to nodulation by rhizobia. *Plant Physiol* **68**, 1144–1149.

Blakely L, Evans T 1979. Cell dynamics studies on the pericycle of radish seedling roots. *Plant Science Letters* **14**, 79–83. ISSN 0304-4211.

Blilou I, Xu J, Wildwater M, Willemsen V, Paponov I, *et al.* 2005. The PIN auxin efflux facilitator network controls growth and patterning in Arabidopsis roots. *Nature* **433**, 39–44.

Casimiro I, Beeckman T, Graham N, Bhalerao R, Zhang H, *et al.* 2003. Dissecting Arabidopsis lateral root development. *Trends Plant Sci* **8**, 165–71.

Compaan B, Yang WC, Bisseling T, Franssen H 2001. Enod40 expression in the pericycle precedes cortical cell division in rhizobium-legume interaction and the highly conserved internal region of the gene does not encode a peptide. *Plant and soil* **230**, 1–8.

Cooper JB, Long SR 1994. Morphogenetic Rescue of Rhizobium meliloti Nodulation Mutants by trans-Zeatin Secretion. *Plant Cell* **6**, 215–225.

Deinum EE, Geurts R, Bisseling T, Mulder BM 2012. Modeling a cortical auxin maximum for nodulation: different signatures of potential strategies. *Front Plant Sci* **3**, 96.

Dello Ioio R, Nakamura K, Moubayidin L, Perilli S, Taniguchi M, *et al.* 2008. A genetic framework for the control of cell division and differentiation in the root meristem. *Science* **322**, 1380–4.

den Camp RHMO, Mita SD, Lillo A, Cao Q, Limpens E, *et al.* 2011. A phylogenetic strategy based on a legume-specific whole genome duplication yields symbiotic cytokinin type-a response regulators. *Plant Physiol* **157**, 2013–2022.

Ding Z, Galván-Ampudia CS, Demarsy E, Langowski L, Kleine-Vehn J, *et al.* 2011. Light-mediated polarization of the pin3 auxin transporter for the phototropic response in arabidopsis. *Nat Cell Biol* **13**, 447–452.

Dolan L, Janmaat K, Willemsen V, Linstead P, Poethig S, *et al.* 1993. Cellular organisation of the arabidopsis thaliana root. *Development* **119**, 71–84.

Doyle J 1994. Phylogeny of the legume family: an approach to understanding the origins of nodulation. *Annual Review of Ecology and Systematics* **25**, 325–349. ISSN 0066-4162.

Fortin MC, Pierce FJ, Poff KL 1989. The pattern of secondary root formation in curving roots of Arabidopsis thaliana (L.) Heynh. *Plant Cell Environ* **12**, 337–9.

Friml J, Yang X, Michniewicz M, Weijers D, Quint A, *et al.* 2004. A pinoid-dependent binary switch in apical-basal pin polar targeting directs auxin efflux. *Science* **306**, 862–865.

Galweiler L, Guan C, Muller A, Wisman E, Mendgen K, *et al.* 1998. Regulation of polar auxin transport by AtPIN1 in Arabidopsis vascular tissue. *Science* **282**, 2226–30.

Garnett P, Steinacher A, Stepney S, Clayton R, Leyser O 2010. Computer simulation: the imaginary friend of auxin transport biology. *Bioessays* **32**, 828–35.

Gonzalez-Rizzo S, Crespi M, Frugier F 2006. The medicago truncatula cre1 cytokinin receptor regulates lateral root development and early symbiotic interaction with sinorhizobium meliloti. *Plant Cell* **18**, 2680–2693.

Grieneisen VA, Scheres B 2009. Back to the future: evolution of computational models in plant morphogenesis. *Curr Opin Plant Biol* **12**, 606–14.

Grieneisen VA, Xu J, Maree AF, Hogeweg P, Scheres B 2007. Auxin transport is sufficient to generate a maximum and gradient guiding root growth. *Nature* **449**, 1008–13.

Hirota A, Kato T, Fukaki H, Aida M, Tasaka M 2007. The auxin-regulated AP2/EREBP gene PUCHI is required for morphogenesis in the early lateral root primordium of Arabidopsis. *Plant Cell* **19**, 2156–68.

Hirsch A 1992. Developmental biology of legume nodulation. *New Phytologist* **122**, 211–237. ISSN 0028-646X.

Hirsch AM, Bhuvaneswari TV, Torrey JG, Bisseling T 1989. Early nodulin genes are induced in alfalfa root outgrowths elicited by auxin transport inhibitors. *Proc Natl Acad Sci U S A* **86**, 1244–8.

Jones AR, Kramer EM, Knox K, Swarup R, Bennett MJ, *et al.* 2009. Auxin transport through non-hair cells sustains root-hair development. *Nat Cell Biol* **11**, 78–84.

Jones KM, Kobayashi H, Davies BW, Taga ME, Walker GC 2007. How rhizobial symbionts invade plants: the Sinorhizobium-Medicago model. *Nature Reviews Microbiology* **5**, 619–633. ISSN 1740-1526.

Jonsson H, Krupinski P 2010. Modeling plant growth and pattern formation. *Curr Opin Plant Biol* **13**, 5–11.

Kleine-Vehn J, Dhonukshe P, Swarup R, Bennett M, Friml J 2006. Subcellular trafficking of the arabidopsis auxin influx carrier aux1 uses a novel pathway distinct from pin1. *The Plant Cell Online* **18**, 3171–3181.

Kramer EM 2008. Computer models of auxin transport: a review and commentary. *J Exp Bot* **59**, 45–53.

Laplaze L, Benkova E, Casimiro I, Maes L, Vanneste S, *et al.* 2007. Cytokinins act directly on lateral root founder cells to inhibit root initiation. *Plant Cell* **19**, 3889–900.

Larkin PJ, Gibson JM, Mathesius U, Weinman JJ, Gartner E, *et al.* 1996. Transgenic white clover. Studies with the auxin-responsive promoter, GH3, in root gravitropism and lateral root development. *Transgenic Res* **5**, 325–35.

Laskowski M, Grieneisen VA, Hofhuis H, Hove CA, Hogeweg P, *et al.* 2008. Root system architecture from coupling cell shape to auxin transport. *PLoS Biol* **6**, e307.

Libbenga K, Harkes P 1973. Initial proliferation of cortical cells in the formation of root nodules in pisum sativum l. *Planta* **114**, 17–28.

Lillo A 2012. *Co-option of pre-existing pathways during Rhizobium-legume symbiosis evolution*. Ph.D. thesis, Wageningen University.

Ljung K, Bhalerao RP, Sandberg G 2001. Sites and homeostatic control of auxin biosynthesis in Arabidopsis during vegetative growth. *Plant J* **28**, 465–74.

Lohar DP, VandenBosch KA 2005. Grafting between model legumes demonstrates roles for roots and shoots in determining nodule type and host/rhizobia specificity. *J Exp Bot* **56**, 1643–50.

Malamy JE, Benfey PN 1997. Organization and cell differentiation in lateral roots of Arabidopsis thaliana. *Development* **124**, 33–44.

Mallory T, Chiang S, Cutter E, Gifford E 1970. Sequence and pattern of lateral root formation in 5 selected species. *American Journal of Botany* **57**, 800–&. ISSN 0002-9122.

Mano Y, Nemoto K 2012. The pathway of auxin biosynthesis in plants. *J Exp Bot* **63**, 2853–2872.

Marchant A, Bhalerao R, Casimiro I, Eklof J, Casero PJ, *et al.* 2002. AUX1 promotes lateral root formation by facilitating indole-3-acetic acid distribution between sink and source tissues in the Arabidopsis seedling. *Plant Cell* **14**, 589–97.

Marhavy P, Bielach A, Abas L, Abuzeineh A, Duclercq J, *et al.* 2011. Cytokinin modulates endocytic trafficking of pin1 auxin efflux carrier to control plant organogenesis. *Dev Cell* **21**, 796–804.

Masucci JD, Schiefelbein JW 1994. The rhd6 mutation of arabidopsis thaliana alters root-hair initiation through an auxin- and ethylene-associated process. *Plant Physiol* **106**, 1335–1346.

Mathesius U, Schlaman HR, Spaink HP, Of Sautter C, Rolfe BG, *et al.* 1998. Auxin transport inhibition precedes root nodule formation in white clover roots and is regulated by flavonoids and derivatives of chitin oligosaccharides. *Plant J* **14**, 23–34.

Mergaert P, Nikovics K, Kelemen Z, Maunoury N, Vaubert D, *et al.* 2003. A novel family in Medicago truncatula consisting of more than 300 nodule-specific genes coding for small, secreted polypeptides with conserved cysteine motifs. *Plant Physiol* **132**, 161–73.

Michniewicz M, Zago MK, Abas L, Weijers D, Schweighofer A, *et al.* 2007. Antagonistic regulation of PIN phosphorylation by PP2A and PINOID directs auxin flux. *Cell* **130**, 1044–56.

Mitchison G 1980. The dynamics of auxin transport. *Proceedings of the Royal Society of London. Series B. Biological Sciences* **209**, 489–511.

Murray JD, Karas BJ, Sato S, Tabata S, Amyot L, *et al.* 2007. A cytokinin perception mutant colonized by Rhizobium in the absence of nodule organogenesis. *Science* **315**, 101–4.

Pacios-Bras C, Schlaman HR, Boot K, Admiraal P, Langerak JM, *et al.* 2003. Auxin distribution in Lotus japonicus during root nodule development. *Plant Mol Biol* **52**, 1169–80.

Paponov IA, Teale WD, Trebar M, Blilou I, Palme K 2005. The pin auxin efflux facilitators: evolutionary and functional perspectives. *Trends Plant Sci* **10**, 170–177.

Petersson SV, Johansson AI, Kowalczyk M, Makoveychuk A, Wang JY, *et al.* 2009. An auxin gradient and maximum in the Arabidopsis root apex shown by high-resolution cell-specific analysis of IAA distribution and synthesis. *Plant Cell* **21**, 1659–68.

Pitts RJ, Cernac A, Estelle M 1998. Auxin and ethylene promote root hair elongation in arabidopsis. *Plant J* **16**, 553–560.

Plet J, Wasson A, Ariel F, Le Signor C, Baker D, *et al.* 2011. MtCRE1-dependent cytokinin signaling integrates bacterial and plant cues to coordinate symbiotic nodule organogenesis in Medicago truncatula. *Plant J* **65**, 622–633.

Rolfe B, Djordjevic M, Weinman J, Mathesius U, Pittock C, *et al.* 1997. Root morphogenesis in legumes and cereals and the effect of bacterial inoculation on root development. *Plant and Soil* **194**, 131–144. ISSN 0032-079X. Meeting on Opportunities for Biological Nitrogen Fixation in Rice and Other Non-Legumes, Natl Inst Biotechnol & Genet Engn, Falsalabad, Pakistan, Oct 13-15, 1996.

Steinacher A, Leyser O, Clayton RH 2012. A computational model of auxin and ph dynamics in a single plant cell. *J Theor Biol* **296**, 84–94.

Swarup R, Friml J, Marchant A, Ljung K, Sandberg G, *et al.* 2001. Localization of the auxin permease aux1 suggests two functionally distinct hormone transport pathways operate in the arabidopsis root apex. *Genes & Development* **15**, 2648–2653.

Swarup R, Kargul J, Marchant A, Zadik D, Rahman A, *et al.* 2004. Structure-function analysis of the presumptive arabidopsis auxin permease aux1. *The Plant Cell Online* **16**, 3069–3083.

Swarup R, Kramer EM, Perry P, Knox K, Leyser HM, *et al.* 2005. Root gravitropism requires lateral root cap and epidermal cells for transport and response to a mobile auxin signal. *Nat Cell Biol* **7**, 1057–65.

Takanashi K, Sugiyama A, Yazaki K 2011. Involvement of auxin distribution in root nodule development of Lotus japonicus. *Planta* **234**, 73–81. ISSN 0032-0935.

Timmers A, Auriac M, Truchet G 1999. Refined analysis of early symbiotic steps of the rhizobium-medicago interaction in relationship with microtubular cytoskeleton rearrangements. *Development* **126**, 3617–3628.

Tirichine L, Sandal N, Madsen LH, Radutoiu S, Albrektsen AS, *et al.* 2007. A gain-of-function mutation in a cytokinin receptor triggers spontaneous root nodule organogenesis. *Science* **315**, 104–107. ISSN 0036-8075.

Woodward AW, Bartel B 2005. Auxin: regulation, action, and interaction. *Ann Bot* **95**, 707–35.

Yang WC, de Blank C, Meskiene I, Hirt H, Bakker J, *et al.* 1994. Rhizobium nod factors reactivate the cell cycle during infection and nodule primordium formation, but the cycle is only completed in primordium formation. *Plant Cell* **6**, 1415–26.

6 Tables and figures

Parameter	(Default) value	Description
D_C	300 $\mu m^2 s^{-1}$	Auxin diffusion constant inside cells [Laskowski et al. 2008]
D_W	44 $\mu m^2 s^{-1}$	Auxin diffusion constant in apoplast [Jones et al. 2009]
$P_{out,high}$	20 $\mu m s^{-1}$	Effective efflux permeability, high value [Grieneisen et al. 2007, Laskowski et al. 2008]
$P_{out,low}$	5 $\mu m s^{-1}$	Effective efflux permeability, low value [Grieneisen et al. 2007, Laskowski et al. 2008]
$P_{out,bg}$	1 $\mu m s^{-1}$	Effective efflux permeability, background value (due to misplaced PINs) [Grieneisen et al. 2007, Laskowski et al. 2008]
P_{in}	20 $\mu m s^{-1}$	Effective influx permeability [Grieneisen et al. 2007, Laskowski et al. 2008]
C_v	concentration	The average auxin concentration in the vascular tissue is normalized to 1 C_v. (Strictly speaking, C_v is not a parameter.)
p	$0; 10^{-4} C_v \mu m^{-3} s^{-1}$	Auxin production rate; Default: no production. Estimates for reasonable rates based on [Ljung et al. 2001], scaled relative to total concentrations [Marchant et al. 2002].
l	100 μm	Cell length
w_C	20 μm	Width of cortical cells
w_x	10 μm	Width of other cells
d_W	0.2 μm	Wall thickness [Jones et al. 2009]
d_p	2 μm	Pixel size for the cells' interior
t	0.5, 1, 2.5 s	Integration time step (dependent on interval between measurements)

Table 1: Overview of model parameters. See methods and [Deinum et al. 2012] for explanation.

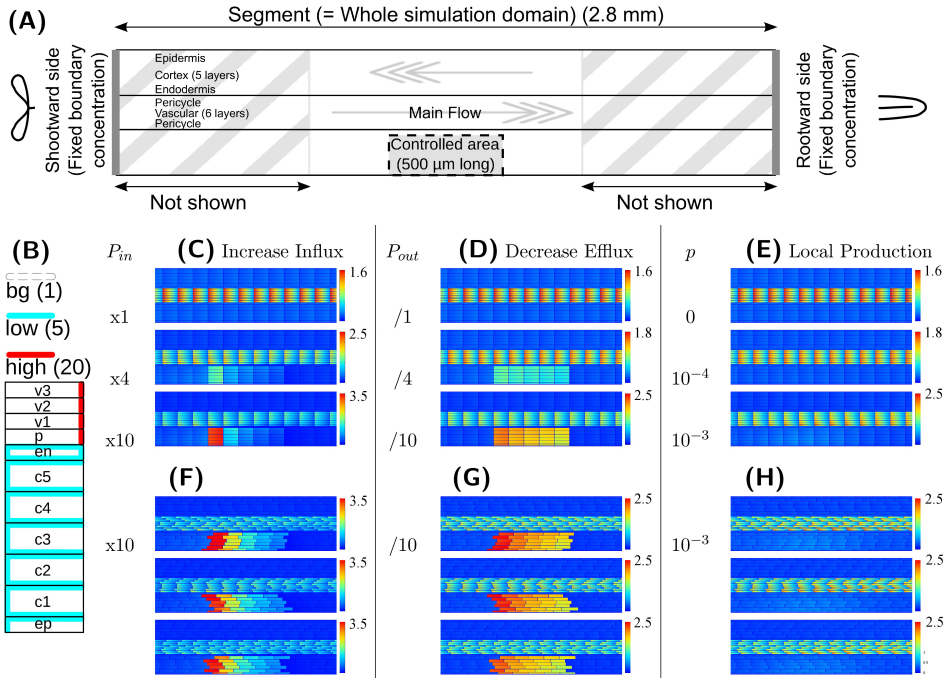

Figure 1: Different mechanisms for local auxin accumulation leave different signatures. General setup is a root segment representative of the susceptible zone of module legumes *Lotus* and *Medicago* (A). The distribution of PIN proteins (B) gives rise to net auxin fluxes as indicated in A. PINs are modelled using effective efflux permeabilities P_{out} with three starting levels: "bg" ($1\mu m/s$), "low" ($5\mu m/s$) and "high" ($20\mu m/s$), following Laskowski et al. [2008]. A five cells long block of cells, consisting of all five cortical layers and the epidermis is designated *"controlled area"*. Changes are applied to these cells: increase of the effective influx permeability, Infl↓ (C,F), decrease of the effective efflux permeability, Efflux↓ (D,G), or local auxin production, Prod↑ (E,H), with indicated factors or rates. Note that Infl↓ results in a much stronger accumulation on the right/downstream side of the controlled area, whereas Efflux↓ results in more homogeneous accumulation. Randomly generated root segments (F-H) with an average cell length of 100 μm, normally distributed with $\sigma = 4\mu m$, show that the observed patterns do not depend on the square layout of the default segments. Concentration ranges are adapted for maximum visibility, all ranging from 0 to the maximum (in C_v) indicated with each subfigure. Figure after Deinum *et al. Front. plant sci.* 2012.

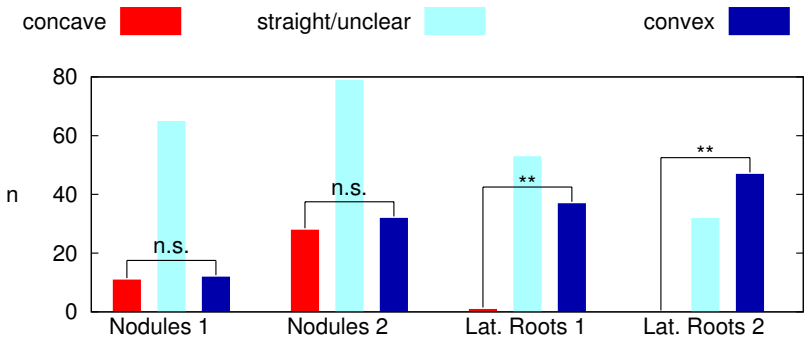

Figure 2: Root nodule position is insensitive to root curvature. Numbers of root nodules and lateral roots and their position with respect to root curvature: concave ("inside", red) or convex ("outside", blue) side of bend parts, or on straight parts (cyan) of the root. Root nodules showed no significant bias for either side of the root curve (p=1, p=0.699), whereas lateral roots showed a very strong bias towards the convex side (p=2.84e-10, p=1.42e-14). On both plates, lateral roots occurred relatively more often on bend regions than lateral roots (42% vs. 26%, p=0.014 and 59% vs. 43%, p=0.011). Roots were bend by exposing *Medicag truncatula* A17 plants on large square plates to varying gravitropic fields. Results of two representative plates with slightly different growth conditions and rotation regimes.

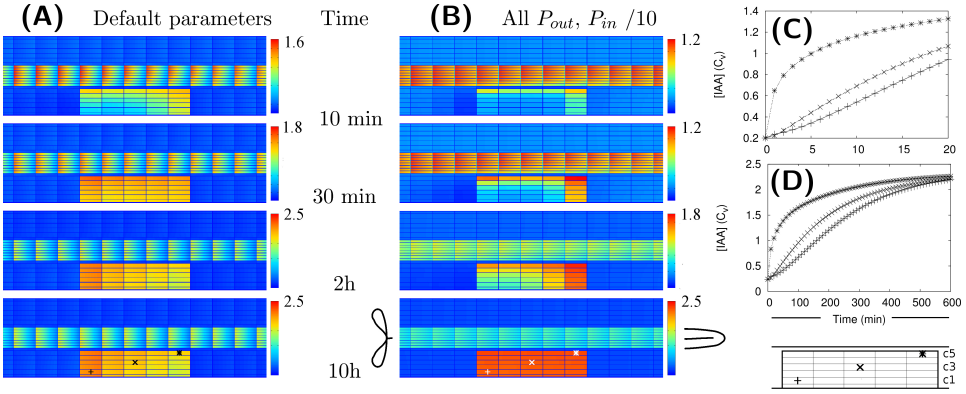

Figure 3: Auxin accumulation following an efflux reduction starts from the inner cortex, closest to the main auxin source. At T=0s, the efflux in the controlled area is reduced by a factor 10 (Efflux↓). The concentration is shown as heat maps at designated time points (A,B) and using time traces of the concentration in three designated cells in the controlled area (C,D). Both with default parameters (A,C) and with "slowed down" parameters (B,D), the auxin concentration increases first in the inner cortex and towards the left of the controlled area. These locations are closest to the vascular tissue and influx from unaffected cortex, respectively. "Slowed down": a 10 fold reduction of all influx and efflux parameters in the whole segment, prior to any change. Figure after Deinum *et al. Front. plant sci.* 2012.

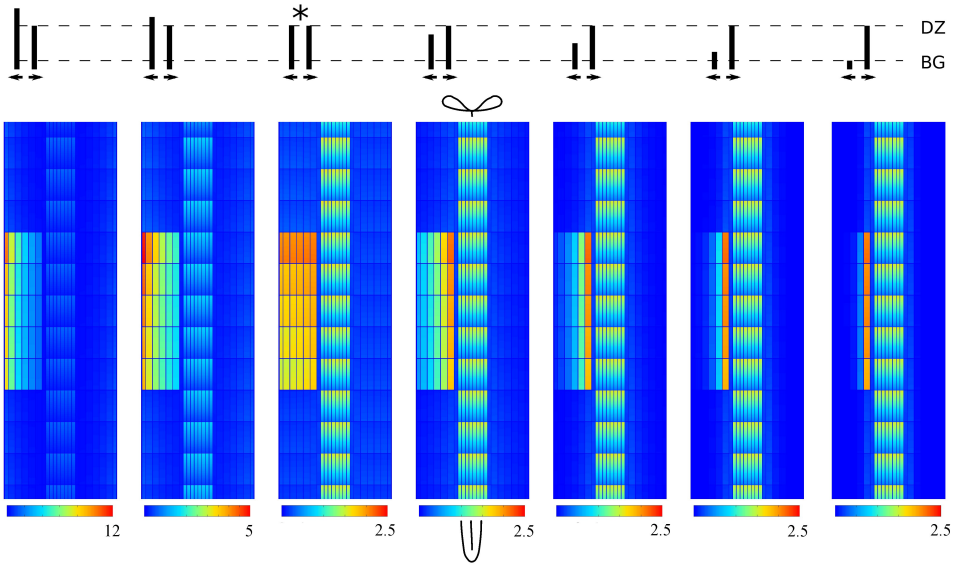

Figure 4: Changes in cortical PINs can shift the lateral location of the induced cortical auxin maximum. The maxima are all induced by the same decrease of efflux. The segments differ only in the effective efflux permeability of the outward faces of the cortical cell, ranging from 140% to 20% of the inward value, as indicated by the cartoon on top. The default layout, 100%, is indicated with *. In all cases the highest concentration in the controlled area is above the vascular concentration C_v. Figure after Deinum *et al. Front. plant sci.* 2012.

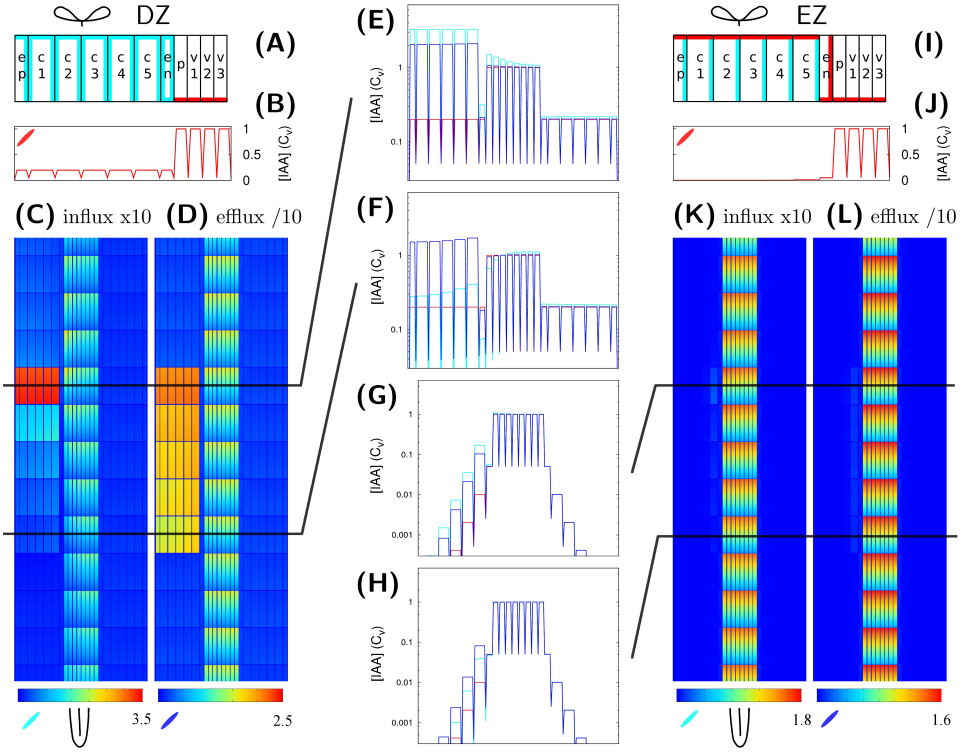

Figure 5: Local auxin accumulation in different zones of the root. The same changes, Infl↓ and Efflˇ are applied in different zones of the root, with strikingly different effect on auxin accumulation. The only difference between the root segments is the PIN layout (A,I), "DZ" (A-F) and "EZ" (G-L) as based on Laskowski et al. [2008]. The EZ PIN layout results in a much lower cortical auxin concentration (c.f. J,B). Consequently, much less auxin accumulates in the controlled area after Infl↓ (K vs. C) or Efflˇ (L vs. D) with the EZ layout. Transverse concentration profiles (E-H), plotted on a logarithmic scale for visibility, show that with both changes (Infl↓: cyan, Efflˇ: blue) the resulting profile in the controlled area resembles the original profile (red) in shape. Figure after Deinum *et al. Front. plant sci.* 2012.